Deng, H., Kusky, T., Bozurt, E., Chen, C., Wang, L., Dong, Z., and Meng, J., 2023, Sr-Nd-Ca isotopic variations of Cenozoic calc-alkaline and alkaline volcanic rocks above a slab tear in Western Anatolia, Turkey: GSA Bulletin, https://doi.org/10.1130/B36672.1.

Supplemental Material

Supplemental Text S1. Corresponding detailed descriptions of the analytical methods.

Figure S1. (a) SiO2 versus Na2O + K2O classification diagram from Middlemost (1994); (b) Zr/TiO2 versus Nb/Y classification from Winchester and Floyd (1977); (c) SiO2 versus K2O diagram.

Figure S2. Variation diagrams of $\delta^{44/40}Ca$ values versus LOI contents.

Figure S3. Variation diagrams of CaO, Al_2O_3 and Eu/Eu* versus SiO_2 for the Gördes dacites.

Figure S4. Variation diagrams of SiO_2, Nb/Nb* and La/Sm_{cn} versus $^{87}Sr/^{86}Sr_i$ for the Gördes dacites.

Figure S5. Variation diagrams of MgO, TFe_2O_3, CaO and CaO/Al_2O_3 versus SiO_2 for the Kula basalts.

Figure S6. Variation diagrams of SiO_2, La/Sm_{cn}, Nb/Nb* versus εNd (t) and 1/Sr versus $(^{87}Sr/^{86}Sr)_i$ for the Kula basalts.

Figure S7. Variation diagrams of La/Sm versus Sm/Yb.

Figure S8. Selected cathodoluminescence images and U-Pb concordia diagrams of analyzed zircons of dacites.

Table S1. SHRIMP U–Pb data for zircons from Gördes dacites.

Table S2. Major and trace elemental compositions of dacites and basalts.

Table S3. (a) Modeling calculation of Ca isotope fractionation during partial melting of spinel peridotite, (b) modeling calculation of Ca isotope fractionation during partial melting of garnet peridotite, and (c) modeling calcium isotope fractionation during partial melting of garnet pyroxenite.

Table S4. Measured and recommended trace element concentrations (ppm) for AGV-2, BHVO-2, BCR-2 and RGM2.

Table S5. Whole rock Sr-Nd compositions and calculations of basalts and dacites.

Supporting Material for

Sr-Nd-Ca isotopic variations of Cenozoic calc-alkaline and alkaline volcanic rocks above a slab tear in Western Anatolia, Turkey

Hao Deng[1], Timothy Kusky[1*], Erdin Bozurt[2], Chunfei Chen[3,1], Lu Wang[1], Ziyu Dong[1], Jiannan Meng[1],*

[1] State Key Laboratory of Geological Processes and Mineral Resources, Center for Global Tectonics, School of Earth Sciences, China University of Geosciences, Wuhan 430074, China
[2] Department of Geological Engineering, Middle East Technical University, TR−06800 Ankara, Turkey
[3] ARC Centre of Excellence for Core to Crust Fluid Systems, Dept. of Earth and Environmental Sciences, Macquarie University, North Ryde, New South Wales 2109, Australia

Text S1. Corresponding detailed descriptions of the analytical methods

1.1.Zircon U-Pb dating

Zircon grains were extracted by heavy-liquid and magnetic methods, and were further purified by hand-picking under a binocular micro-scope. Photomicrographs and cathodoluminescence images were taken to examine their internal structures and to select the optimum positions for analysis. U-Pb zircon analyses were undertaken on a SHRIMP-II (sensitive high-resolution ion microprobe) instrument at the Beijing SHRIMP Centre (National Science and Technology Infrastructure), in the Institute of Geology at the Chinese Academy of Geological Sciences in Beijing (China). Detailed analytical procedures follow the method of Williams (1998). Data that are listed in

Table S1, were processed and assessed using the SQUID1.0 and ISOPLOT software of Ludwig (2003).

1.2. Major element analyses of whole rock

Whole-rock samples were crushed in a corundum jaw crusher (to 60 meshes). About 60 g of each sample was powdered in an agate ring mill to less than 200 meshes. Major element analyses of whole rock were conducted on XRF (Primus II, Rigaku, Japan) at the Wuhan Sample solution Analytical Technology Co., Ltd., Wuhan, China. The detailed sample-digesting procedure was as follows: (1) Sample powder (200 mesh) were placed in an oven at 105 ℃ for drying of 12 hours; (2) ~1.0g dried sample was accurately weighted and placed in the ceramic crucible and then heated in a muffle furnace at 1000℃ for 2 hours. After cooling to 400℃, this sample was placed in the drying vessel and weighted again in order to calculate the loss on ignition (LOI). (3) 0.6 g sample powder was mixed with 6.0 g cosolvent (Li2B4O7 : LiBO2 : LiF = 9:2:1) and 0.3 g oxidant (NH4NO3) in a Pt crucible, which was placed in the furnace at1150℃ for 14 min. Then, this melting sample was quenched with air for 1 min to produce flat discs on the fire brick for the XRF analyses.

1.3. Trace element analyses of whole rock

Trace element analysis of whole rock were conducted on Agilent 7700e ICP-MS at the Wuhan Sample Solution Analytical Technology Co., Ltd., Wuhan, China. The detailed sample-digesting procedure was as follows: (1) Sample powder (200 mesh) were placed in an oven at 105 ℃ for drying of 12 hours; (2) 50 mg sample powder was accurately weighed and placed in a Teflon bomb; (3) 1 ml HNO_3 and 1 ml HF were slowly added into the Teflon bomb; (4) Teflon bomb was putted in a stainless steel pressure jacket and heated to 190 ℃ in an oven for >24 hours; (5) After cooling, the Teflon bomb was opened and placed on a hotplate at 140 ℃ and evaporated to incipient dryness, and then 1 ml HNO_3 was added and evaporated to dryness again; (6) 1 ml of HNO_3, 1 ml of MQ water and 1 ml internal standard solution of 1ppm In were added, and the Teflon bomb was resealed and placed in the oven at 190 ℃ for >12 hours; (7)

The final solution was transferred to a polyethylene bottle and diluted to 100 g by the addition of 2% HNO_3.

1.4. Scheme for Sr isotope ratio analyses using MC-ICP-MS

All chemical preparations were performed on class 100 work benches within a class 1000 over-pressured clean laboratory. **Sample digestion:** (1) Sample powder (200 mesh) were placed in an oven at 105 ℃ for drying of 12 hours; (2) 50-200 mg sample powder was accurately weighed and placed in an Teflon bomb; (3) 1-3 ml HNO_3 and 1-3 ml HF were added into the Teflon bomb; (4) Teflon bomb was putted in a stainless steel pressure jacket and heated to 190 ℃ in an oven for >24 hours; (5) After cooling, the Teflon bomb was opened and placed on a hotplate at 140 ℃ and evaporated to incipient dryness, and then 1 ml HNO_3 was added and evaporated to dryness again; (6) The sample was dissolved in 1.5 mL of 2.5 M HCl. **Column chemistry:** After centrifugation, the supernatant solution was loaded into an ion-exchange column packed with AG50W resin. After complete draining of the sample solution, columns were rinsed with 2.5 M HCl to remove undesirable matrix elements. Finally, the Sr fraction was eluted using 2.5 M HCl and gently evaporated to dryness prior to mass-spectrometric measurement. The residue was rinsed with 10 mL of 4.0 M HCl and then the REE fraction was eluted using 10 ml of 4.0 M HCl. The REE solution was used to separate the Nd fraction by the Nd-column method.

For the Rb-rich sample, after the separation of the common ion-exchange column, the Sr fraction was separated again by the Sr-specific resin. The solution was first converted to the HNO_3 media (3 M HNO_3). Then the solution was loaded into the Sr-specific resin and pre-conditioned with 6 M HCl and 3 M HNO_3. After complete draining of the sample solution, columns were rinsed with 3 M HNO_3 to remove undesirable matrix elements. Finally, Sr was eluted using MQ H_2O and gently evaporated to dryness prior to mass-spectrometric measurement.

Sr isotope analyses were performed on a Neptune Plus MC-ICP-MS (Thermo Fisher Scientific, Dreieich, Germany) at the Wuhan Sample Solution Analytical Technology Co., Ltd, Hubei, China. The Neptune Plus, a double focusing MC-ICP-

MS, was equipped with seven fixed electron multiplier ICs, and nine Faraday cups fitted with 10^{11} Ω resistors. The faraday collector configuration of the mass system was composed of an array from L4 to H3 to monitor $^{83}Kr^{+}$、$^{167}Er^{++}$、$^{84}Sr^{+}$、$^{85}Rb^{+}$、$^{86}Sr^{+}$、$^{173}Yb^{++}$、$^{87}Sr^{+}$、$^{88}Sr^{+}$. The large dry interface pump (120 m^3 hr^{-1} pumping speed) and newly designed X skimmer cone and Jet sample cone were used to increase the instrumental sensitivity. Sr single element solution from Alfa (Alfa Aesar, Karlsruhe, Germany) was used to optimize instrument operating parameters. An aliquot of the international standard solution of 200 μg L^{-1} NIST SRM 987 was used regularly for evaluating the reproducibility and accuracy of the instrument. Typically, the signal intensities of ^{88}Sr in NIST SRM 987 were > ~4.0 V. The Sr isotopic data were acquired in the static mode at low resolution. The routine data acquisition consisted of ten blocks of 10 cycles (4.194 s integration time per cycle). The total time of one measurement lasted about 7 minutes.

The exponential law, which initially was developed for TIMS measurement (Russell et al. 1978) and remains the most widely accepted and utilized with MC-ICP-MS, was used to assess the instrumental mass discrimination in this study. Mass discrimination correction was carried out via internal normalization to a $^{88}Sr/^{86}Sr$ ratio of 8.375209 (Lin et al. 2016). The interference elements Ca, Rb, Er, Yb have been completely separated by the exchange resin process. The remaining interferences of $^{83}Kr^{+}$、$^{85}Rb^{+}$、$^{167}Er^{++}$、$^{173}Yb^{++}$ were corrected based on the mothed described by Lin et al. (2016). One international NIST SRM 987 standard was measured every ten samples analyzed. Analyses of the NIST SRM 987 standard solution yielded $^{87}Sr/^{86}Sr$ ratio of 0.710244±22 (2SD, n=32), which is identical within error to their published values (0.710241±12, Thirlwall, 1991). In addition, the USGS reference materials BCR-2 (basalt) and RGM-2 (rhyolite) yielded results of 0.705034±14 (2SD, n=4) and 0.704192±10 (2SD, n=4) for $^{87}Sr/^{86}Sr$, respectively, which is identical within error to their published values (Li et al. 2012).

1.5. Scheme for Nd isotope ratio analyses using MC-ICP-MS

All chemical preparations were performed on class 100 work benches within a class 1000 over-pressured clean laboratory. Column chemistry: The REE solution from the Sr-column method was evaporated to incipient dryness, and taken up with 0.18 M HCl. The converted REE solution was loaded into an ion-exchange column packed with LN resin. After complete draining of the sample solution, columns were rinsed with 0.18 M HCl to remove undesirable matrix elements. Finally, the Sr fraction was eluted using 0.3 M HCl and gently evaporated to dryness prior to mass-spectrometric measurement.

Nd isotope analyses were performed on a Neptune Plus MC-ICP-MS (Thermo Fisher Scientific, Dreieich, Germany) at the Wuhan Sample Solution Analytical Technology Co., Ltd, Hubei, China. The Neptune Plus, a double focusing MC-ICP-MS, was equipped with seven fixed electron multiplier ICs, and nine Faraday cups fitted with 10^{11} Ω resistors. The faraday collector configuration of the mass system was composed of an array from L4 to H4 to monitor $^{142}Nd^{+}$、$^{143}Nd^{+}$、$^{144}Nd^{+}$、$^{145}Nd^{+}$、$^{146}Nd^{+}$、$^{147}Sm^{+}$、$^{148}Nd^{+}$、$^{149}Sm^{+}$、$^{150}Nd^{+}$. The large dry interface pump (120 m^3 hr^{-1} pumping speed) and newly designed X skimmer cone and Jet sample cone were used to increase the instrumental sensitivity. Nd single element solution from Alfa (Alfa Aesar, Karlsruhe, Germany) was used to optimize instrument operating parameters. An aliquot of the international standard solution of 200 μg L^{-1} JNdi-1 was used regularly for evaluating the reproducibility and accuracy of the instrument. Typically, the signal intensities of $^{144}Nd^{+}$ in JNdi-1 were > ~2.5 V. The Nd isotopic data were acquired in the static mode at low resolution. The routine data acquisition consisted of ten blocks of 10 cycles (4.194 s integration time per cycle). The total time of one measurement lasted about 7 min.

The exponential law, which initially was developed for TIMS measurement (Russell et al. 1978) and remains the most widely accepted and utilized with MC-ICP-MS, was used to assess the instrumental mass discrimination in this study. Mass discrimination correction was carried out via internal normalization to a $^{146}Nd/^{144}Nd$ ratio of 0.7219 (Lin et al. 2016). The interference elements Sm have been completely separated by the exchange resin process. The remaining interferences of $^{144}Sm^{+}$ were

corrected based on the mothed described by Lin et al. (2016). One JNdi-1 standard was measured every ten samples analyzed. Analyses of the JNdi-1 standard yielded $^{143}Nd/^{144}Nd$ ratio of 0.512118±15 (2SD, n=31), which is identical within error to their published values (0.512115±07, Tanaka et al., 2000). In addition, the USGS reference materials BCR-2 (basalt) and RGM-2 (rhyolite) yielded results of 0.512644±15 (2SD, n=6) and 0.512810±15 (2SD, n=4) for $^{143}Nd/^{144}Nd$, respectively, which is identical within error to their published values (Li et al. 2012).

Collectively, the major and trace elemental data of the analyzed samples are given in Table S2. The results of standard analyses and recommended values are given in Table S3. The analytical data of Rb-Sr and Sm-Nd isotopes are listed in Table S4.

1.6. Calcium isotope analyses

12 samples of early Miocene volcanic rocks from the Gördes basin and 10 samples of Quaternary Kula basalts were selected for calcium isotopes analyses. All chemical preparations were performed on class 100 work benches within a class 1000 over-pressured clean laboratory. **Sample digestion:** (1) Sample powder (200 mesh) were placed in an oven at 105 ℃ for drying of 12 hours; (2) 10 - 50 mg sample powder was accurately weighed and placed in an Teflon bomb; (3) 1 ml HNO_3 and 1 ml HF were added into the Teflon bomb; (4) Teflon bomb was putted in a stainless steel pressure jacket and heated to 190 ℃ in an oven for at least 24 hours; (5) After cooling, the Teflon bomb was opened and placed on a hotplate at 140 ℃ and evaporated to incipient dryness, and then 1 ml HNO_3 was added and evaporated to dryness again; (6) The sample was dissolved in 10 mL of 4 M $HHNO_3$. An aliquot sample solution containing 40 µg Ca was loaded onto the pre-cleaned PFA column which filled with 250 µl DGA resin. All the sample matrices were removed by 4 mol L-1 HNO_3 while quantitative recovery (>99 %) of Ca was achieved by the elution of MQ-H_2O. The collected Ca fractions were evaporated to dryness and re-dissolved in 2 % HNO_3 to obtain 10 ppm Ca solution prior to MC-ICP-MS analysis. The total procedural blank was no more than 20 ng which is negligible compared to the digestions.

Calcium isotopes analyses were performed on a Neptune Plus MC-ICP-MS (Thermo Fisher Scientific, Dreieich, Germany) at the WSSATC. A "wet" plasma, using a quartz dual cyclonic-spray chamber and an Savillex 50 μL min^{-1} PFA MicroFlow Teflon nebulizer (Elemental ScientificInc., U.S.A.), was utilized to measure Ca isotopes. The large dry interface pump (120 m^3 hr^{-1} pumping speed) and newly designed X skimmer cone and Jet sample cone were used to increase the instrumental sensitivity. Typically, the signal intensities of $^{44}Ca^{+}$ in 10 ppm sample solution were > 5 V. Cross-contamination between samples was eliminated by washing the sample-introduction system with 5% HNO_3 for 2-3 min between each measurement until the ^{44}Ca signal is less than 1 mV. Medium resolution mode was used to resolve polyatomic interference, such as $^{40}Ar^{1}H^{2+}$and $^{14}N^{3+}$. The instrumental drift was corrected by the standard-sample bracketing technique. All the Ca isotopic compositions were reported relative to a reference standard by using δ-notation: $\delta^{44/42}Ca_{ref} = [^{44}Ca/^{42}Ca_{sample}/^{44}Ca/^{42}Ca_{ref} -1] \times 1000$. All Ca isotopic values ($\delta^{44/42}Ca$) in this study are then converted to $\delta^{44/40}Ca$ using a factor of 2.048 calculated by the mass dependent fractionation law (Heuser et al., 2016). An in-house Alfa Ca standard solution (Lot: 9192737) was used as bracketing reference standard. However, in order to achieve better comparability of published Ca isotope data, all Ca isotope results were reported relative to commonly used reference standard NIST SRM 915a by adding a conversion factor 0.58 (the $\delta^{44/42}Ca_{SRM915a}$ value of Alfa Ca). Each sample solution has been measured multiple times (≥3), and the two times standard deviation is reported as the analytical uncertainty.

The long-term (>3 months) average $\delta^{44/42}Ca_{SRM915a}$ of NIST 915a is 0.001 ± 0.058‰ (2SD, n = 155) indicated that the reproducibility of our instrument is better than 0.06‰ (2SD). Three reference materials (BHVO-2, BCR-2 and seawater) and two duplicate samples were processed as unknowns to assess accuracy and reproducibility. The analyzed $\delta^{44/42}Ca_{SRM915a}$ values of BHVO-2, BCR-2 and seawater are 0.36 ± 0.02 ‰ (2SD, n = 3), 0.39 ± 0.03 ‰ (2 SD, n = 3) and 0.90 ± 0.04‰ (2SD, n = 3), respectively. These results are consistent with previous studies within analytical uncertainty, conforming the accuracy of our analytical method for Ca isotopes in geological samples (Amini et al., 2009; Feng et al., 2018; Heuser and Eisenhauer, 2008;

Kang et al., 2017; Li et al., 2018). Results of calcium compositions of all samples and standards are listed in Table 1.

2. *Descriptions of zircon U-Pb geochronology*

All zircons derived from the dacites are characterized by weak oscillatory zoning and low luminescence in CL images, consistent with their igneous origin. Thirteen zircons from sample DH822 have high contents of Th (125-390 ppm) and U (597-1499 ppm) with high Th/U (0.17-0.31) ratios. They yield a weighted mean age of 18.19 ± 0.16 Ma (MSWD = 1.09) (Fig. S8). Twelve zircons from sample DH922 have high contents of Th (102-576 ppm) and U (479-2347 ppm) with high Th/U (0.17-0.36) ratios. They yield a weighted mean age of 18.20 ± 0.18 Ma (MSWD = 0.8) (Fig. S8).

3. *Selected model parameters and partition coefficient values for partial melting modelling*

The CaO content of spinel peridotite is 3.54 wt.% (McDonough and Sun, 1995). Initial mineral modal abundance and melting mode of spinel peridotite were adopted from Niu (1997), whereas those of garnet peridotite adopted from Davis et al. (2011) and Walter (1998), respectively. Initial CaO content of minerals of garnet peridotite was taken from Davis et al. (2011). Partition coefficient values (D) for Ca between minerals and basaltic melt of spinel peridotite are adopted from Adam and Green (2006). Partition coefficients for garnet peridotite were calculated from Davis et al. (2011). The initial CaO content and modal abundance of the garnet pyroxenite for modeling calculation are from Gréau et al. (2011). Partition coefficients for garnet pyroxenite are from Pertermann et al. (2004). Detailed calculations can be seen in Table S5.

References

Adam, J., Green, T., 2006. Trace element partitioning between mica-and amphibole-bearing garnet lherzolite and hydrous basanitic melt: 1. Experimental results and the investigation of controls on partitioning behaviour. Contributions to Mineralogy and Petrology 152, 1-17.

Amini, M., Eisenhauer, A., Böhm, F., Holmden, C., Kreissig, K., Hauff, F., Jochum, K.P., 2009. Calcium isotopes (δ44/40Ca) in MPI-DING reference glasses, USGS rock powders and various rocks: Evidence for Ca isotope fractionation in terrestrial silicates. Geostandards and Geoanalytical Research 33, 231-247.

Aldanmaz, E., Pearce, J.A., Thirlwall, M., Mitchell, J., 2000. Petrogenetic evolution of late Cenozoic, post-collision volcanism in western Anatolia, Turkey. Journal of volcanology and geothermal research, 102(1-2): 67-95.

Davis, F., Hirschmann, M., Humayun, M., 2011. The composition of the incipient partial melt of garnet peridotite at 3 GPa and the origin of OIB. Earth and Planetary Science Letters 308, 380-390.

Feng, L., Zhou, L., Yang, L., Zhang, W., Wang, Q., Tong, S., Hu, Z., 2018. A rapid and simple single-stage method for Ca separation from geological and biological samples for isotopic analysis by MC-ICP-MS. Journal of Analytical Atomic Spectrometry 33, 413-421.

Gréau, Y., Huang, J.-X., Griffin, W.L., Renac, C., Alard, O., O'Reilly, S.Y., 2011. Type I eclogites from Roberts Victor kimberlites: Products of extensive mantle metasomatism. Geochimica et Cosmochimica Acta 75, 6927-6954.

Heuser, A., Eisenhauer, A., 2008. The calcium isotope composition (δ44/40Ca) of NIST SRM 915b and NIST SRM 1486. Geostandards and Geoanalytical Research 32, 27-32.

Li, C.F., Li, X.H., Li, Q.L., Guo, J.H. and Yang, Y.H., 2012. Rapid and precise determination of Sr and Nd isotopic ratios in geological samples from the same filament loading by thermal ionization mass spectrometry employing a single-step separation scheme. Analytica Chimica Acta, 727 (10), 54–60.

Li, C., Ripley, E.M., 2010. The relative effects of composition and temperature on olivine-liquid Ni partitioning: Statistical deconvolution and implications for petrologic modeling. Chemical Geology 275, 99-104.

Li, M., Lei, Y., Feng, L., Wang, Z., Belshaw, N.S., Hu, Z., Liu, Y., Zhou, L., Chen, H., Chai, X., 2018. High-precision Ca isotopic measurement using a large geometry high resolution MC-ICP-MS with a dummy bucket. Journal of Analytical Atomic Spectrometry 33, 1707-1719.

Lin, J., Liu Y.S., Yang Y.H.and Hu Z.C., 2016, Calibration and correction of LA-ICP-MS and LA-MC-ICP-MS analyses for element contents and isotopic ratios. Solid Earth Sciences, 1, 5–27.

McDonough, W.F., Sun, S.-S., 1995. The composition of the Earth. Chemical Geology 120, 223-253.

Niu, Y., 1997. Mantle melting and melt extraction processes beneath ocean ridges: evidence from abyssal peridotites. Journal of Petrology 38, 1047-1074.

Pertermann, M., Hirschmann, M.M., Hametner, K., Günther, D., Schmidt, M.W., 2004. Experimental determination of trace element partitioning between garnet and silica-rich liquid during anhydrous partial melting of MORB-like eclogite. Geochemistry, Geophysics, Geosystems 5 (5).

Russell, W.A., Papanastassiou, D.A. and Tombrello, T.A., 1978. Ca isotope fractionation on the earth and other solar system materials. Geochim. Cosmochim. Acta, 42 (8), 1075–1090.

Takahashi, E., 1985. Origin of basaltic magma-Implications from peridotite melting experiments and an olivine fractionation model. Bull. Volcanol. Soc. Japan 30, S17-S40.

Tanaka, T., Togashi, S., Kamioka, H., Amakawa, H., Kagami, H., Hamamoto, T., et al., 2000. Jndi-1: a neodymium isotopic reference in consistency with lajolla neodymium. Chemical Geology, 168 (168), 279-281.

Thirlwall, M.F., 1991. Long-term reproducibility of multicollector sr and nd isotope ratio analysis. Chemical Geology, 94 (2), 85–104.

Walter, M.J., 1998. Melting of garnet peridotite and the origin of komatiite and depleted lithosphere. Journal of Petrology 39, 29-60.

Weis, D., Kieffer, B., Maerschalk, C., Barling, J., Jong, J. D., Williams, G. A., et al., 2006. High-precision isotopic characterization of USGS reference materials by TIMS and MC-ICP-MS. Geochemistry Geophysics Geosystems, 7 (8), 139-149.

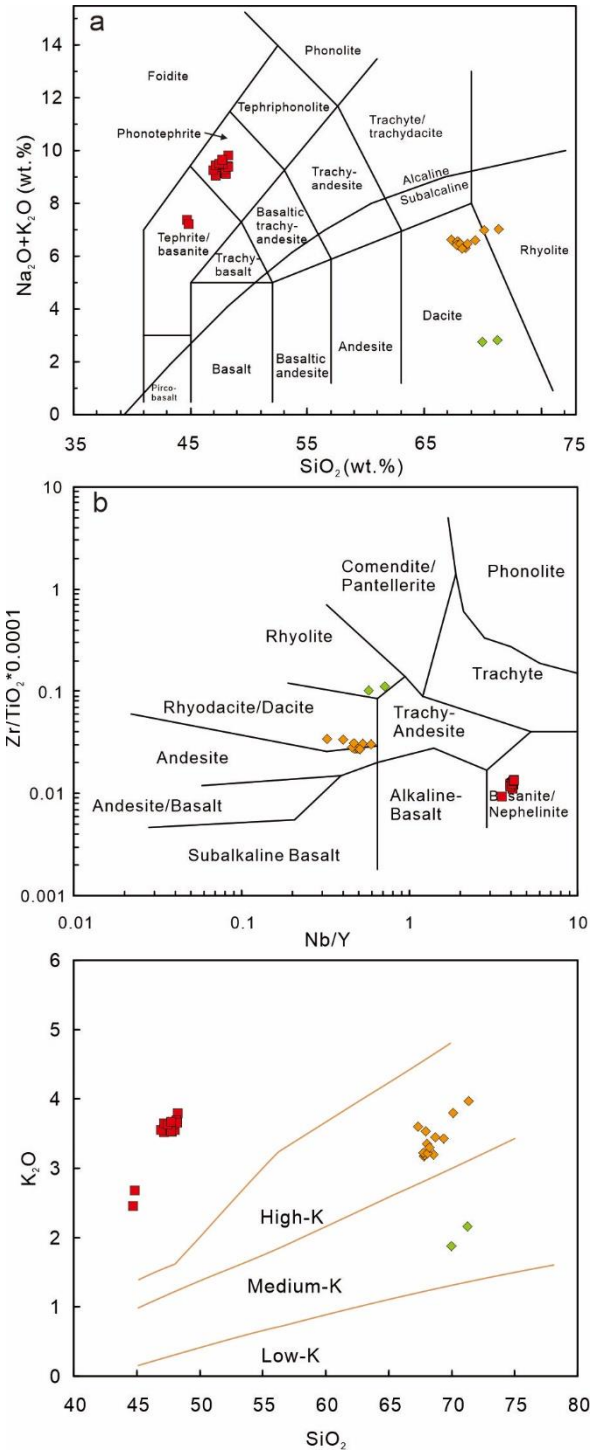

Fig. S1. (a) SiO_2 versus $Na_2O + K_2O$ classification diagram from Middlemost (1994); (b) Zr/TiO_2 versus Nb/Y classification from Winchester and Floyd (1977); (c) SiO_2 versus K_2O diagram.

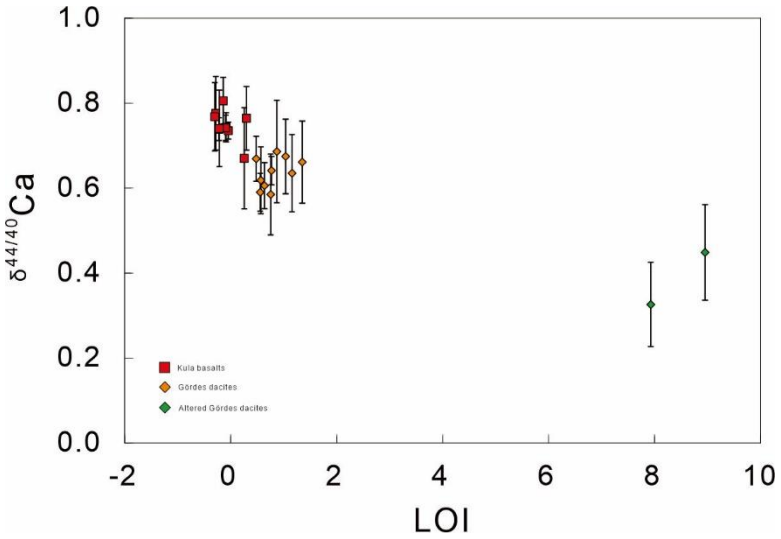

Fig. S2. Variation diagrams of $\delta^{44}/^{40}Ca$ values versus LOI contents.

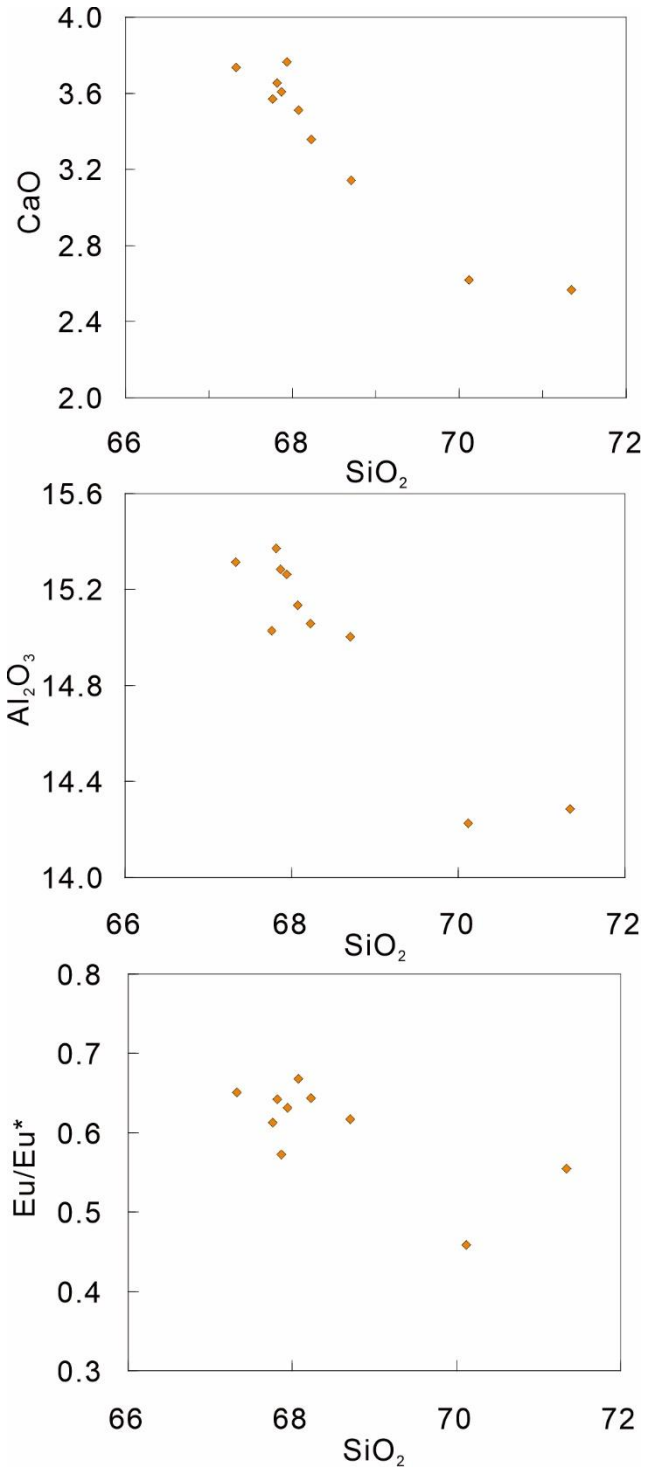

Fig. S3. Variation diagrams of CaO, Al_2O_3 and Eu/Eu* versus SiO_2 for the Gördes dacites.

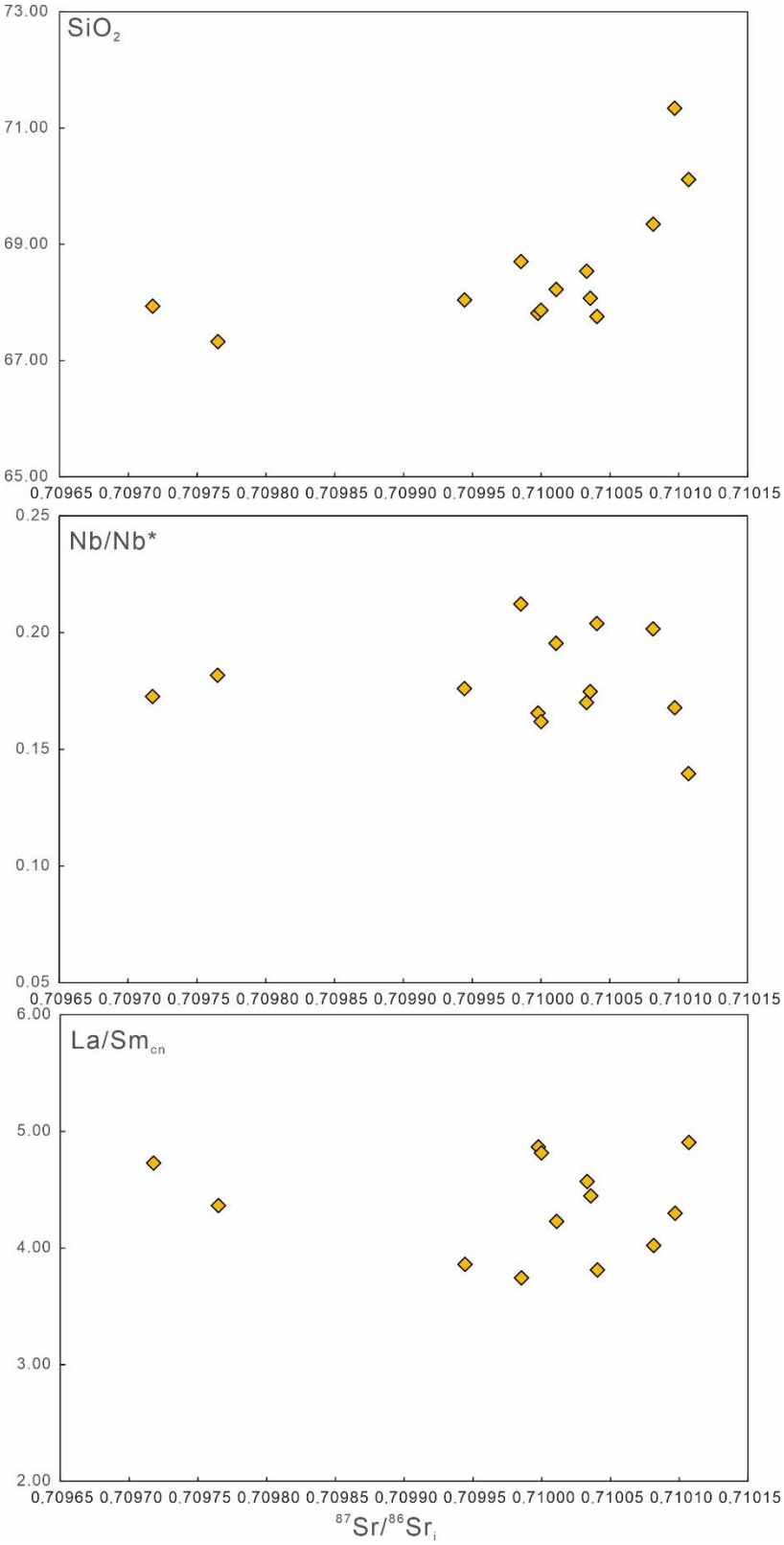

Fig. S4. Variation diagrams of SiO_2, Nb/Nb* and La/Sm_{cn} versus $^{87}Sr/^{86}Sr_i$ for the Gördes dacites.

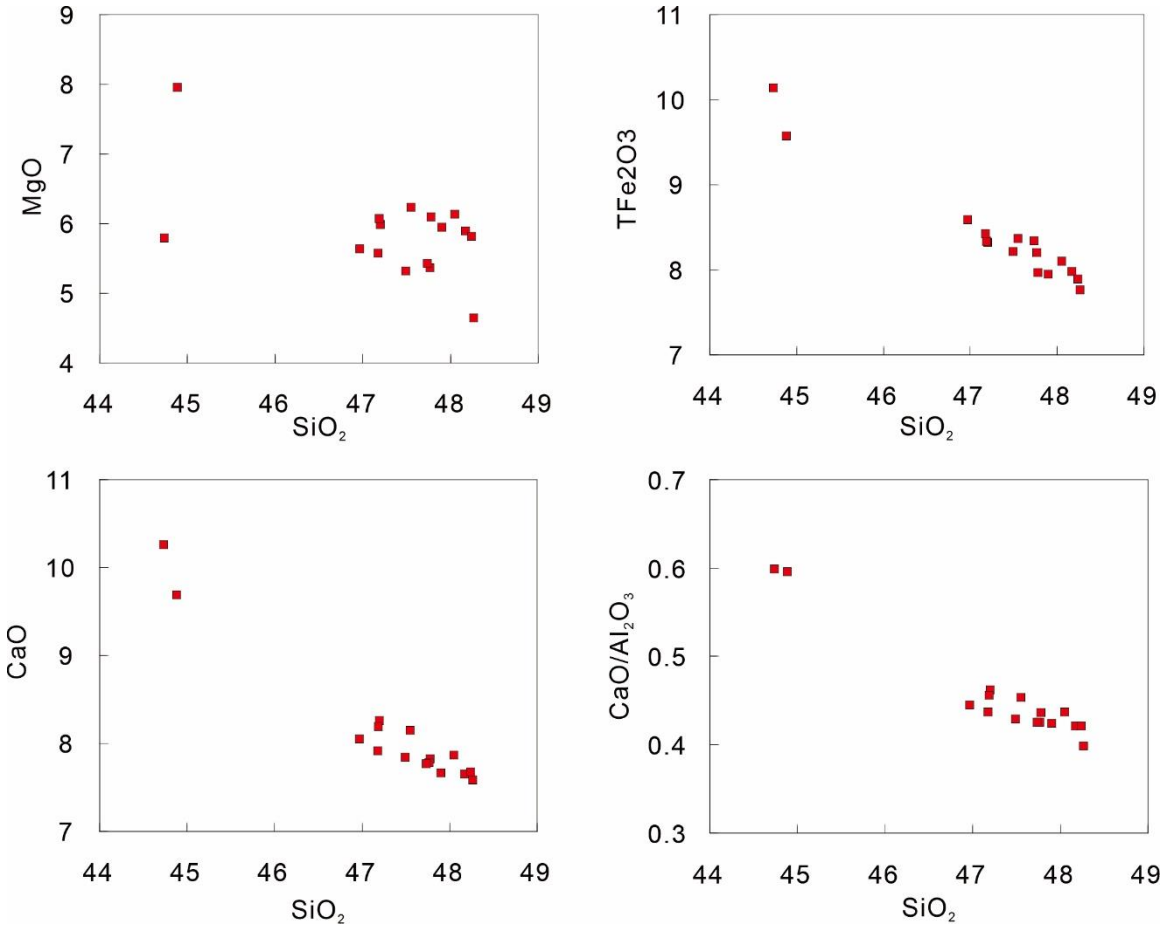

Fig. S5. Variation diagrams of MgO, TFe_2O_3, CaO and CaO/Al_2O_3 versus SiO_2 for the Kula basalts.

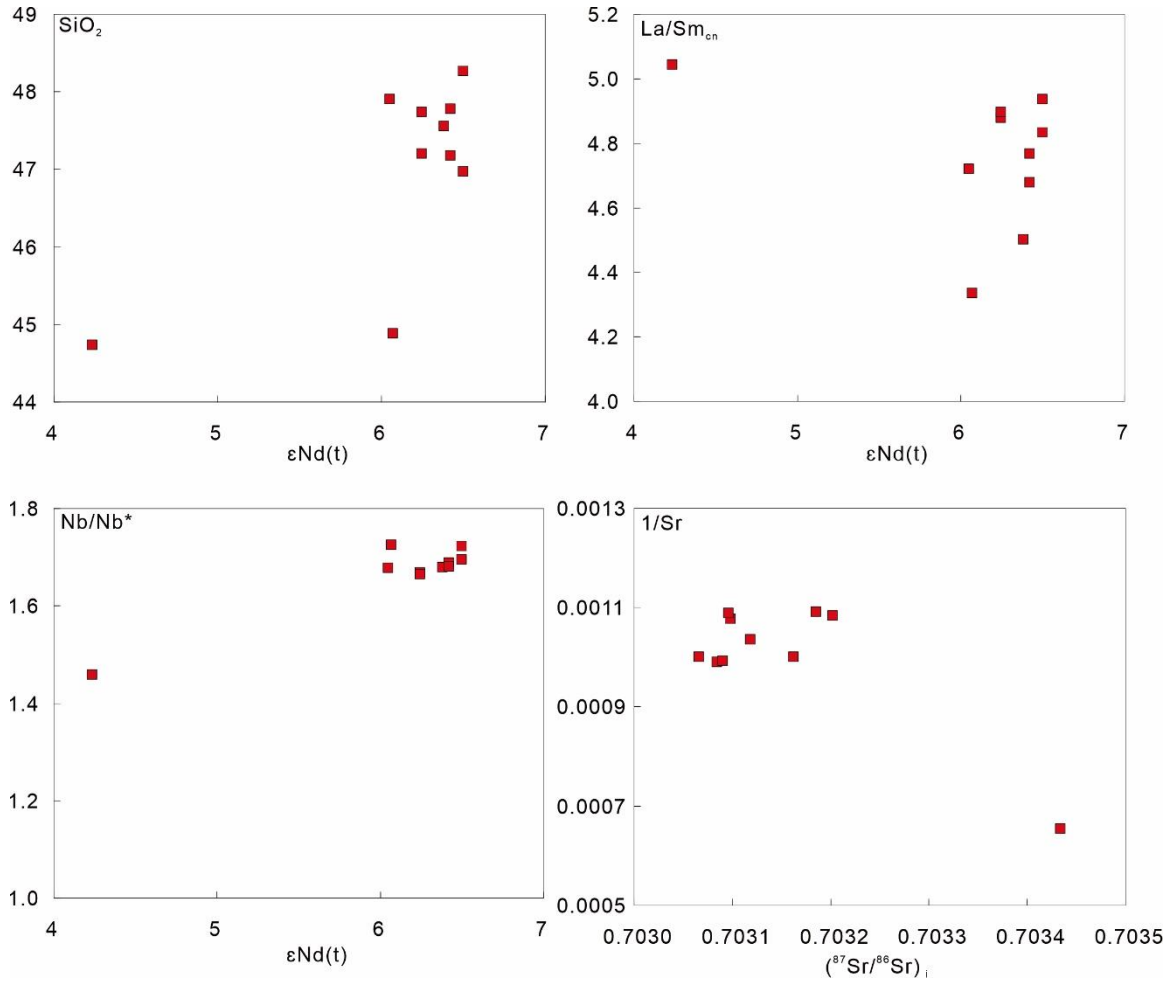

Fig. S6. Variation diagrams of SiO_2, La/Sm_{cn}, Nb/Nb* versus εNd (t) and 1/Sr versus $(^{87}Sr/^{86}Sr)_i$ for the Kula basalts.

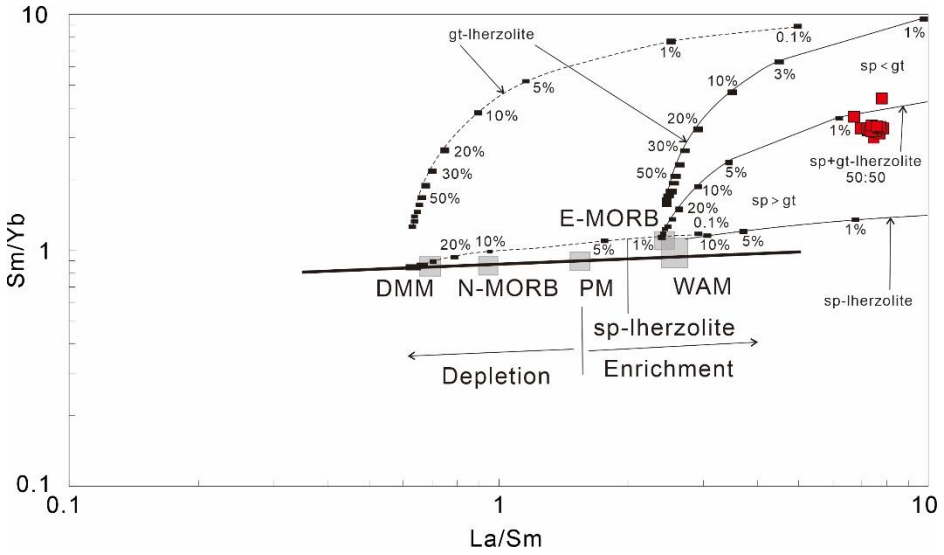

Fig. S7. Variation diagrams of La/Sm versus Sm/Yb (adopted from Aldanmaz et al., 2000).

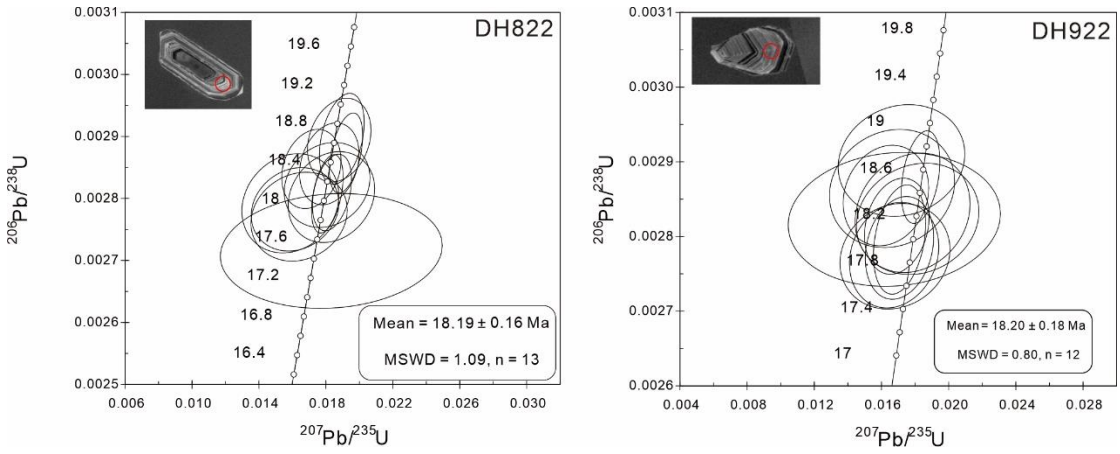

Fig. S8. Selected cathodoluminescence images and U-Pb concordia diagrams of analyzed zircons of dacites.

Table S1. SHRIMP U–Pb data for zircons from Gördes dacites

Spot	% $^{206}P_c$	ppm U	ppm Th	$^{232}Th/^{238}U$	ppm ^{206}Pb*	$^{207}Pb/^{206}Pb$	err	$^{207}Pb/^{235}U$	err	$^{206}Pb/^{238}U$	err	Err corr	206Pb/238U	err
Sample 822DH dacite														
822-01	0.69	688	135	0.20	1.7	0.0412	11.9	0.0159	12.0	.0028	1.9	.157	18.0	0.3
822-02	1.83	630	129	0.21	1.5	0.0489	23.8	0.0183	23.9	.0027	2.2	.094	17.5	0.4
822-03	1.14	954	294	0.32	2.3	0.0421	10.6	0.0162	10.7	.0028	1.6	.149	17.9	0.3
822-04	0.72	1487	390	0.27	3.7	0.0436	6.7	0.0171	6.8	.0028	1.5	.217	18.3	0.3
822-05	0.00	1045	288	0.29	2.5	0.0467	3.1	0.0181	3.4	.0028	1.5	.432	18.1	0.3
822-06	0.00	597	163	0.28	1.5	0.0475	4.3	0.0189	4.7	.0029	1.7	.359	18.6	0.3
822-07	0.75	794	172	0.22	1.9	0.0429	11.5	0.0164	11.6	.0028	1.7	.147	17.8	0.3
822-08	0.00	1099	311	0.29	2.7	0.0485	3.1	0.0192	3.4	.0029	1.5	.434	18.5	0.3
822-09	1.04	1141	197	0.18	2.8	0.0464	9.2	0.0181	9.4	.0028	1.6	.171	18.2	0.3
822-10	0.47	949	217	0.24	2.4	0.0471	6.5	0.0188	6.7	.0029	1.5	.231	18.6	0.3
822-11	0.71	642	125	0.20	1.6	0.0474	9.1	0.0183	9.3	.0028	1.7	.185	18.0	0.3
822-12	0.45	939	292	0.32	2.3	0.0462	6.3	0.0182	6.4	.0029	1.5	.237	18.4	0.3
822-13	0.40	1499	376	0.26	3.6	0.0474	3.9	0.0184	4.2	.0028	1.5	.345	18.1	0.3
Sample 922DH dacite														
922-1	0.96	603	133	0.23	1.5	0.0421	14.7	0.0166	14.8	.0029	1.8	.123	18.4	0.3
922-2	1.11	560	148	0.27	1.4	0.0438	10.3	0.0168	10.5	.0028	1.7	.161	17.9	0.3
922-3	0.63	1592	576	0.37	3.8	0.0443	5.7	0.0171	6.0	.0028	1.7	.288	18.0	0.3
922-4	1.02	1233	206	0.17	3.1	0.0413	10.2	0.0163	10.3	.0029	1.6	.151	18.4	0.3
922-5	1.47	582	104	0.18	1.4	0.0431	24.8	0.0168	24.9	.0028	2.1	.084	18.2	0.4
922-6	0.25	2347	519	0.23	5.8	0.0462	3.9	0.0183	4.1	.0029	1.4	.344	18.5	0.3
922-7	0.91	736	155	0.22	1.9	0.0430	14.4	0.0172	14.5	.0029	1.7	.118	18.7	0.3
922-8	0.91	855	255	0.31	2.1	0.0445	7.7	0.0171	7.9	.0028	1.6	.207	17.9	0.3
922-9	0.70	1129	326	0.30	2.7	0.0436	7.4	0.0169	7.5	.0028	1.5	.201	18.1	0.3
922-10	0.96	479	102	0.22	1.2	0.0457	12.5	0.0179	12.6	.0028	1.9	.147	18.2	0.3

922-11	0.56	906	185	0.21	2.2	0.0466	13.1	0.0182	13.3	.0028	1.7	.131	18.2	0.3
922-12	1.34	989	246	0.26	2.4	0.0439	12.7	0.0168	12.9	.0028	1.7	.131	17.9	0.3

Errors are 1-sigma and Pb* indicates the radiogenic portions.

Data were ^{204}Pb corrected, using measured values.

% discordance=% discordance defined as [(^{206}Pb/^{238}Pb age)/(^{207}Pb/^{206}Pb age)]×100.

Table S2. Major and trace elemental compositions of dacites and basalts

Sample No	919DH	920DH	820DH	821DH	822DH	824DH	921DH	922DH	923DH	924DH	926DH	927DH	928DH	929DH	930DH
Rock type	Altered dacite			Dacite											
SiO2	71.26	69.98	67.33	67.94	67.82	67.87	68.04	70.12	68.54	67.76	69.35	68.07	68.23	68.71	71.34
TiO2	0.09	0.08	0.49	0.50	0.49	0.52	0.51	0.35	0.50	0.48	0.45	0.48	0.50	0.49	0.36
Al2O3	12.11	12.61	15.31	15.26	15.37	15.28	15.29	14.23	14.89	15.03	15.07	15.13	15.06	15.00	14.29
TFe2O3	0.99	0.41	3.73	3.82	3.58	3.70	3.63	2.72	3.64	3.56	3.32	3.52	3.58	3.52	2.85
MnO	0.00	0.01	0.08	0.07	0.08	0.08	0.07	0.08	0.06	0.07	0.08	0.09	0.06	0.06	0.06
MgO	0.82	0.94	1.32	1.43	1.58	1.82	1.51	1.25	1.63	1.60	1.38	1.65	1.82	1.51	1.19
CaO	3.33	3.68	3.74	3.77	3.65	3.61	3.29	2.62	3.43	3.57	3.31	3.51	3.36	3.14	2.57
Na2O	0.66	0.89	3.03	3.00	3.39	3.24	3.05	3.19	3.12	3.22	3.17	3.25	3.00	3.03	3.06
K2O	2.16	1.87	3.60	3.53	3.17	3.19	3.35	3.80	3.20	3.22	3.43	3.21	3.30	3.45	3.97
P2O5	0.02	0.02	0.11	0.11	0.10	0.14	0.12	0.08	0.11	0.15	0.11	0.12	0.15	0.16	0.09
LOI	7.93	8.95	0.77	0.76	0.48	0.57	1.36	1.04	0.66	0.87	0.44	0.56	1.16	1.35	0.64
SUM	99.36	99.45	99.50	100.19	99.72	100.01	100.23	99.46	99.78	99.53	100.11	99.60	100.22	100.42	100.41
Li	6.57	5.09	43.80	44.4	50.9	49.5	50.6	53.1	49.3	46.9	50.3	47.6	46.3	44.4	60.3
Be	3.16	3.59	2.63	2.57	2.80	2.80	2.99	2.90	2.81	2.65	2.89	2.74	2.77	2.56	3.13
Sc	2.68	2.40	11.19	10.8	9.93	10.2	9.70	7.51	10.2	9.84	8.78	9.62	9.17	9.69	7.71
V	4.44	4.56	81.75	81.0	44.2	46.0	45.2	35.1	46.1	43.4	40.0	43.6	42.5	44.4	35.2
Cr	40.7	31.2	105.62	114	96.2	96.3	60.1	78.9	116	92.1	89.2	103	78.9	98.5	127
Co	0.92	0.75	10.03	10.1	8.85	9.55	16.6	7.15	8.41	9.08	8.11	8.84	8.94	8.11	7.42
Ni	4.74	6.29	16.22	17.0	9.14	9.68	8.51	8.85	10.4	9.04	9.52	10.8	14.8	9.34	10.1
Cu	2.34	1.83	9.91	9.78	7.37	8.05	7.38	5.88	7.88	7.53	6.37	7.81	7.53	7.07	6.93
Zn	21.6	14.7	44.74	44.6	41.0	44.4	106	34.7	43.3	42.9	39.4	41.4	40.4	38.7	35.0
Ga	13.5	13.9	16.87	16.8	16.7	16.9	16.9	15.8	16.6	16.4	16.6	16.7	16.4	15.7	15.9
Rb	156	120	125.83	125	117	118	119	138	112	113	121	117	114	118	134
Sr	429	691	316.85	311	334	293	281	216	276	290	290	307	268	285	220
Y	27.8	22.1	24.72	24.3	25.6	25.1	38.5	30.8	23.8	24.5	23.5	26.5	23.9	20.7	25.4
Zr	87.2	93.7	134.85	138	136	144	174	118	145	137	139	136	137	149	113
Nb	15.9	15.8	11.91	12.3	12.0	12.4	12.4	12.4	12.1	12.1	12.4	12.0	12.1	12.3	11.8
Sn	3.57	3.74	4.45	4.70	3.54	3.56	2.61	3.68	3.66	2.09	3.32	3.12	2.61	2.55	2.82
Cs	9.29	4.15	7.35	6.37	6.31	5.76	6.00	7.29	6.39	6.23	6.96	6.22	5.12	6.38	9.93

Ba	123	1093	713.17	711	658	689	737	658	641	683	722	715	751	663	625		
La	23.2	22.2	32.76	36.1	37.3	39.8	37.7	42.8	36.1	28.5	29.3	35.1	30.6	27.1	32.6		
Ce	44.3	45.2	61.37	67.8	69.9	74.9	69.2	80.5	68.5	56.9	56.4	67.4	58.3	53.1	62.3		
Pr	5.34	5.15	6.71	7.28	7.26	7.81	7.95	8.22	7.37	6.09	6.01	7.06	6.21	5.74	6.48		
Nd	19.8	19.2	25.04	26.2	26.7	28.7	30.1	29.5	26.3	23.0	22.8	25.9	23.3	21.9	24.1		
Sm	4.38	4.39	4.85	4.92	4.95	5.34	6.31	5.63	5.11	4.83	4.70	5.10	4.67	4.67	4.89		
Eu	0.26	0.25	0.96	0.97	0.97	0.93	1.22	0.80	0.93	0.95	0.91	1.04	0.96	0.87	0.83		
Gd	3.97	4.08	4.17	4.50	4.34	4.60	6.06	5.07	4.51	4.69	4.16	4.48	4.48	3.96	4.30		
Tb	0.66	0.67	0.69	0.65	0.67	0.72	1.02	0.79	0.73	0.73	0.71	0.69	0.75	0.62	0.70		
Dy	4.19	3.90	4.17	4.30	4.16	4.38	6.41	4.88	4.38	4.34	4.28	4.48	4.18	3.66	4.33		
Ho	0.91	0.75	0.88	0.87	0.85	0.84	1.33	0.98	0.86	0.89	0.84	0.93	0.90	0.73	0.87		
Er	2.53	2.15	2.42	2.43	2.45	2.53	3.82	2.89	2.47	2.47	2.42	2.59	2.46	2.12	2.42		
Tm	0.39	0.32	0.37	0.37	0.37	0.39	0.56	0.44	0.36	0.35	0.36	0.38	0.37	0.31	0.37		
Yb	2.62	2.09	2.35	2.37	2.50	2.47	3.61	2.90	2.44	2.44	2.41	2.52	2.44	2.10	2.55		
Lu	0.40	0.31	0.36	0.38	0.37	0.38	0.55	0.45	0.37	0.37	0.38	0.40	0.39	0.34	0.38		
Hf	3.32	3.62	3.95	3.83	3.90	4.14	4.69	3.63	4.19	3.98	4.04	3.96	3.88	4.22	3.42		
Ta	1.48	1.57	1.22	1.25	1.25	1.22	1.26	1.56	1.24	1.21	1.33	1.28	1.24	1.30	1.46		
Tl	0.59	1.10	0.84	0.81	0.79	0.96	0.76	0.83	1.16	0.73	0.73	0.78	0.70	0.72	0.67		
Pb	18.1	21.7	37.49	37.3	34.3	32.8	52.6	39.0	40.2	35.5	37.1	31.1	35.7	34.5	40.7		
Th	29.3	31.0	15.07	16.1	16.2	16.8	15.1	21.2	16.0	14.3	14.8	15.5	14.4	14.1	17.5		
U	4.86	5.46	4.63	4.83	4.29	4.67	4.43	6.03	4.47	3.94	4.17	4.51	4.15	4.39	4.92		
North	38.58319	38.58319	38.92379	38.92379	38.89518	38.89518	38.57195	38°54′39″	38.568889	38.568889	38.568889	38.588056	38.596111	38.596389	38.613611		
East	28.63559	28.63559	28.20033	28.20033	28.11762	28.11762	28.6493	28°11′34″	28.652222	28.652222	28.652222	28.664167	28.677778	28.6775	28.687222		

Table S1. Continued

Sample No	825DH	831DH	836DH	843DH	844DH	912DH	913DH	914DH	915DH	916DH	917DH	918DH	932DH	933DH	935DH	936DH	937DH
Rock type	Basalt																
SiO2	47.96	48.27	48.17	44.74	47.55	47.78	48.05	47.90	48.24	47.20	47.19	44.88	46.97	47.18	47.77	47.49	47.74
TiO2	1.81	1.84	1.79	2.27	1.87	1.79	1.81	1.77	1.76	1.90	1.91	2.32	1.98	1.93	1.86	1.89	1.89
Al2O3	18.21	19.05	18.19	17.14	17.97	17.94	18.01	18.07	18.24	17.88	17.97	16.26	18.09	18.13	18.31	18.28	18.26
TFe2O3	7.97	7.76	7.98	10.14	8.37	7.96	8.10	7.95	7.89	8.32	8.33	9.57	8.59	8.42	8.20	8.21	8.34
MnO	0.14	0.14	0.14	0.16	0.15	0.14	0.14	0.14	0.14	0.15	0.15	0.16	0.15	0.15	0.15	0.15	0.16
MgO	5.63	4.64	5.89	5.79	6.23	6.09	6.14	5.95	5.82	5.99	6.07	7.96	5.63	5.57	5.36	5.32	5.43
CaO	7.68	7.58	7.65	10.26	8.15	7.83	7.86	7.66	7.68	8.26	8.19	9.69	8.05	7.91	7.78	7.84	7.77

Na2O	5.72	6.03	5.72	4.93	5.70	5.65	5.56	5.68	5.74	5.60	5.53	4.55	5.69	5.78	5.95	5.88	6.00
K2O	3.60	3.79	3.68	2.45	3.61	3.52	3.55	3.62	3.65	3.55	3.51	2.67	3.55	3.64	3.53	3.62	3.67
P2O5	0.75	0.77	0.82	1.22	0.78	0.79	0.80	0.80	0.80	0.81	0.80	0.99	0.95	0.91	0.87	0.87	0.88
LOI	-0.25	-0.09	-0.08	0.26	-0.22	-0.05	-0.05	-0.14	-0.34	-0.28	0.04	0.30	-0.10	-0.21	-0.14	-0.22	-0.30
SUM	99.21	99.77	99.94	99.35	100.16	99.44	99.97	99.39	99.60	99.37	99.69	99.35	99.55	99.41	99.65	99.32	99.82
Li	9.37	10.2	10.7	11.9	9.67	10.4	10.3	10.4	10.7	10.3	8.74	6.73	8.36	9.42	9.32	9.19	9.95
Be	2.19	2.36	2.52	2.37	2.34	2.33	2.55	2.44	2.35	2.50	2.37	2.00	2.52	2.44	2.56	2.58	2.68
Sc	16.5	14.8	14.6	16.4	15.8	15.1	15.6	14.9	14.3	16.4	16.6	22.1	15.1	15.0	14.5	14.6	14.3
V	148	144	143	227	155	146	149	146	143	165	162	216	157	155	146	149	147
Cr	147	107	112	88.2	123	143	176	127	126	145	134	175	175	110	128	151	150
Co	28.5	25.1	28.9	35.5	28.6	29.3	30.4	29.0	28.0	31.2	29.3	39.9	28.8	28.8	26.2	27.9	27.0
Ni	62.4	39.7	75.4	32.5	70.1	80.5	85.1	77.8	75.2	70.4	68.5	103	58.1	57.4	55.7	56.5	57.9
Cu	32.6	30.7	32.6	33.4	29.8	32.8	35.2	32.8	31.9	33.2	31.9	40.3	32.8	31.7	31.4	31.8	31.4
Zn	69.1	68.1	69.7	89.6	69.8	69.2	71.2	71.6	69.9	72.9	74.4	79.0	73.7	74.6	72.0	72.1	72.5
Ga	19.5	20.2	19.4	20.6	19.7	19.2	19.9	19.3	19.5	20.2	20.5	19.5	19.9	20.9	20.1	19.9	20.1
Rb	78.1	82.7	82.4	64.6	77.1	79.0	79.3	81.2	82.7	79.9	78.9	87.3	76.2	79.2	76.5	75.5	80.3
Sr	899	929	931	1529	919	923	923	917	934	966	933	1000	999	1010	1008	993	1008
Y	23.3	23.2	23.7	30.8	23.5	23.7	23.9	23.6	23.8	25.0	24.4	27.8	25.8	26.0	25.3	25.5	25.2
Zr	216	225	228	251	218	225	222	222	227	228	223	215	245	254	253	249	254
Nb	91.7	96.4	96.7	127	94.5	96.4	96.7	94.9	98.6	100	98.0	99.2	106	109	107	106	106
Sn	1.81	1.65	1.69	1.81	1.67	1.71	1.74	1.65	1.59	1.63	1.67	1.69	1.76	1.69	1.81	2.02	1.77
Cs	1.31	1.31	1.35	1.18	1.27	1.32	1.28	1.33	1.29	1.31	1.23	1.04	1.17	1.27	1.21	1.25	1.28
Ba	860	895	892	1071	879	899	874	879	898	905	893	963	899	932	928	920	917
La	46.2	47.0	49.4	85.3	47.6	48.3	48.8	48.0	50.1	51.7	49.8	54.2	56.0	56.4	56.1	56.6	55.0
Ce	79.0	80.8	84.4	154	83.4	83.5	84.1	82.9	85.6	89.3	85.8	97.1	94.8	97.3	96.0	96.4	95.0
Pr	8.43	8.44	8.88	16.2	8.92	8.93	8.89	8.98	9.13	9.66	9.28	10.7	10.2	10.6	10.2	10.2	10.0
Nd	32.8	32.5	34.2	62.3	33.9	33.8	33.6	34.1	34.3	35.8	35.0	41.8	39.0	39.1	38.7	38.9	38.6
Sm	6.13	6.27	6.56	10.9	6.82	6.66	6.77	6.57	6.48	6.84	6.73	8.07	7.32	7.64	7.13	7.32	7.25
Eu	1.94	2.03	2.02	3.23	2.07	2.08	2.08	1.90	2.07	2.18	2.19	2.56	2.41	2.38	2.35	2.28	2.32
Gd	5.38	5.49	5.79	8.69	5.69	5.68	5.70	5.61	5.74	5.95	5.79	7.01	6.28	6.23	6.13	6.25	6.06
Tb	0.77	0.81	0.83	1.12	0.81	0.78	0.81	0.81	0.79	0.91	0.83	0.98	0.88	0.88	0.86	0.87	0.88
Dy	4.58	4.68	4.52	6.28	4.61	4.64	4.77	4.60	4.66	5.09	4.70	5.32	5.02	5.05	4.77	5.00	4.84

Ho	0.85	0.87	0.83	1.14	0.85	0.86	0.90	0.84	0.90	0.94	0.92	0.96	0.98	0.97	0.89	0.94	0.91
Er	2.32	2.34	2.36	2.95	2.30	2.35	2.44	2.35	2.33	2.45	2.42	2.62	2.50	2.60	2.51	2.52	2.55
Tm	0.33	0.32	0.33	0.37	0.32	0.32	0.32	0.33	0.32	0.33	0.32	0.35	0.36	0.36	0.35	0.35	0.35
Yb	1.96	2.10	2.08	2.49	2.08	2.08	2.07	2.05	2.09	2.16	2.12	2.21	2.22	2.26	2.18	2.21	2.18
Lu	0.30	0.32	0.31	0.34	0.30	0.31	0.30	0.30	0.30	0.32	0.31	0.32	0.34	0.34	0.33	0.33	0.32
Hf	4.50	4.48	4.44	4.76	4.45	4.44	4.48	4.42	4.44	4.53	4.47	4.58	4.95	5.23	4.88	4.94	4.93
Ta	4.92	5.12	5.30	5.99	5.09	5.16	5.16	5.13	5.34	5.41	5.34	5.35	5.83	6.05	5.90	5.81	5.87
Tl	0.10	0.076	0.085	0.078	0.073	0.094	0.096	0.090	0.097	0.096	0.059	0.12	0.075	0.083	0.12	0.099	0.099
Pb	4.20	6.00	6.30	7.20	4.98	6.24	5.56	5.93	5.83	5.06	4.12	4.00	4.57	4.50	5.16	5.49	4.97
Th	7.43	7.66	7.79	10.2	7.65	7.75	7.43	7.65	7.85	7.99	7.57	7.01	8.06	8.50	8.23	8.19	8.48
U	2.14	2.28	2.35	2.86	2.14	2.43	2.18	2.30	2.33	2.29	2.26	2.08	2.43	2.63	2.38	2.42	2.38
North	38.57416	38.57416	38.57805	38.594722	38.59333	38.586367	38.578197	38.596569	38.606456	38.586708	38.619458	38.778117	38.614711	38.620167	38.637878	38.638119	38.636769
East	28.55361	28.55361	28.55361	28.558333	28.55777	28.703461	28.690011	28.703564	28.699878	28.513625	28.531469	28.538592	28.412781	28.399275	28.419219	28.420522	28.443214

Table S3. Measured and recommended trace element concentrations (ppm) for AGV-2, BHVO-2, BCR-2 and RGM2

Sample no.	BLANK	AGV-2	AGV-2	BHVO-2	BHVO-2	BCR-2	BCR-2	RGM-2	RGM-2	820DH	914DH	927DH	820DH*	914DH*	927DH*
Analysis No.	Sample	Sample	Ref	Sample	Ref	Sample	Ref	Sample	Ref	Sample	Sample	Sample	D*	D*	D*
Li	0.0237	10.0	11.0	4.35	4.80	8.83	9.00	58.8	57.0	43.8	10.4	47.6	44.2	10.6	48.2
Be	0.0000	2.11	2.30	1.05	1.00	2.33		2.54	2.37	2.63	2.44	2.74	2.58	2.48	2.89
Sc	0.0446	12.2	13.0	32.1	32.0	33.8	33.0	4.45	4.40	11.2	14.9	9.62	10.8	15.1	9.48
V	0.1607	116	120	320	317	419	416	11.8	13.0	81.7	146	43.6	80.8	145	42.6
Cr	0.0339	14.9	16.2	291	280	14.8	16.5	2.66	5.90	106	127	103	99.6	131	115
Co	0.0065	15.0	16.0	46.3	45.0	36.8	37.0	2.05	2.00	10.0	29.0	8.84	9.78	28.8	9.09
Ni	0.2105	19.2	20.0	125	119	13.7	13.0	2.52	5.20	16.2	77.8	10.8	15.7	77.8	10.3
Cu	0.0158	48.0	53.0	132	127	21.0	19.7	9.36	9.60	9.91	32.8	7.81	9.90	32.7	8.07
Zn	0.0380	84.3	86.0	108	103	132	133	30.3	32.0	44.7	71.6	41.4	43.8	69.9	41.4
Ga	0.0018	20.6	20.0	21.8	21.7	22.3	23.0	16.6	16.5	16.9	19.3	16.7	16.6	19.4	16.4
Rb	0.0212	67.2	66.3	9.09	9.11	47.3	46.9	149	150	126	81.2	117	125	80.6	115
Sr	0.0872	653	661	400	396	345	340	108	108	317	917	307	317	889	303
Y	0.0078	19.7	20.0	26.1	26.0	36.9	37.0	23.4	23.2	24.7	23.6	26.5	24.2	23.5	25.5
Zr	0.0392	227	230	169	172	184	184	227	220	135	222	136	132	221	142
Nb	0.0033	14.1	14.5	18.6	18.1	12.6	12.6	9.29	9.30	11.9	94.9	12.0	12.2	95.4	12.1
Sn	0.0990	1.81	1.83	1.72	1.70	2.00	2.03	3.37	3.34	4.45	1.65	3.12	4.38	1.70	2.81
Cs	0.0014	1.15	1.16	0.095	0.10	1.10	1.10	9.62	9.60	7.35	1.33	6.22	7.67	1.34	6.31
Ba	0.1632	1116	1130	129	131	668	677	836	810	713	879	715	733	873	729
La	0.0035	38.5	37.9	15.5	15.2	24.7	24.9	23.3	24.0	32.8	48.0	35.1	31.2	47.6	33.3
Ce	0.0091	69.0	68.6	37.5	37.5	53.0	52.9	46.6	47.0	61.4	82.9	67.4	59.6	82.4	63.1
Pr	0.0012	8.10	7.84	5.20	5.35	6.68	6.70	5.28	5.36	6.71	8.98	7.06	6.36	8.70	6.69
Nd	0.0027	30.8	30.5	24.2	24.5	28.2	28.7	19.5	19.0	25.0	34.1	25.9	24.2	33.5	24.9
Sm	0.0017	5.40	5.49	6.22	6.07	6.77	6.58	4.07	4.30	4.85	6.57	5.10	4.96	6.49	5.07
Eu	0.0007	1.58	1.54	2.08	2.07	1.94	1.96	0.63	0.66	0.96	1.90	1.04	1.00	2.05	0.95
Gd	0.0015	4.72	4.52	6.27	6.24	6.57	6.75	3.67	3.70	4.17	5.61	4.48	4.34	5.67	4.22
Tb	0.0008	0.63	0.64	0.95	0.92	1.12	1.07	0.60	0.66	0.69	0.81	0.69	0.70	0.83	0.68
Dy	0.0011	3.63	3.47	5.41	5.31	6.47	6.41	3.81	4.10	4.17	4.60	4.48	4.07	4.54	4.36
Ho	0.0007	0.67	0.65	0.99	0.98	1.32	1.28	0.76	0.82	0.88	0.84	0.93	0.87	0.91	0.94
Er	0.0004	1.91	1.81	2.51	2.54	3.60	3.66	2.34	2.35	2.42	2.35	2.59	2.37	2.32	2.52
Tm	0.0007	0.26	0.26	0.33	0.33	0.54	0.54	0.37	0.37	0.37	0.33	0.38	0.37	0.32	0.41

Yb	0.0011	1.69	1.62	2.07	2.00	3.38	3.38	2.48	2.60	2.35	2.05	2.52	2.36	2.13	2.53
Lu	0.0002	0.25	0.25	0.29	0.27	0.51	0.50	0.38	0.40	0.36	0.30	0.40	0.36	0.31	0.39
Hf	0.0023	5.06	5.00	4.49	4.36	4.87	4.90	6.05	6.20	3.95	4.42	3.96	3.80	4.52	3.99
Ta	0.0008	0.84	0.87	1.14	1.14	0.79	0.78	0.97	0.95	1.22	5.13	1.28	1.31	5.09	1.28
Tl	0.0008	0.31	0.27	0.021	0.058	0.30		1.00	0.93	0.84	0.090	0.78	0.93	0.098	0.87
Pb	0.0032	13.7	13.2	1.60	1.60	10.0	11.0	19.9	19.3	37.5	5.93	31.1	37.5	6.11	31.2
Th	0.0040	6.27	6.10	1.22	1.22	5.88	5.70	14.8	15.1	15.1	7.65	15.5	14.5	7.70	15.2
U	0.0010	1.94	1.86	0.39	0.40	1.66	1.69	5.77	5.80	4.63	2.30	4.51	4.66	2.23	4.49

Analyzed international standard materials include AGV-2, BHVO-2, BCR-2 and RGM2. The recommended value of the standard materials is from http://minerals.cr.usgs.gov/geo_chem_stand/, http://georem.mpch-mainz.gwdg.de/ and Govindaraju G.(1994). D*=duplicate. References: Govindaraju G. Compilation of working values and sample description for 383 geostandards. Geostandards Newslett. 1994,18: 1-158. Liu YS, Zong KQ, Kelemen PB and Gao S, 2008. Geochemistry and magmatic history of eclogites and ultramafic rocks from the Chinese continental scientific drill hole: subduction and ultrahigh-pressure metamorphism of lower crustal cumulates. Chemical Geology, 247: 133-153.

Table S4. Whole rock Sr-Nd compositions and calculations of basalts and dacites

Sample no.	Rock type	Rb	Sr	T(Ma)	$^{87}Rb/^{86}Sr$	$^{87}Sr/^{86}Sr$	±2σ	$(^{87}Sr/^{86}Sr)_i$	Sm	Nd	$^{147}Sm/^{144}Nd$	$^{143}Nd/^{144}Nd$	±2σ	$\varepsilon_{Nd}(t)$	$(^{143}Nd/^{144}Nd)_i$
831DH	Basalt	82.7	929	0.236	0.258	0.703099	0.000011	0.70310	6.27	32.5	0.117	0.512971	0.000005	6.5	0.512971
843DH	Basalt	64.6	1529	0.236	0.122	0.703434	0.000009	0.70343	10.9	62.3	0.106	0.512855	0.000004	4.2	0.512855
844DH	Basalt	77.1	919	0.236	0.243	0.703097	0.000008	0.70310	6.82	33.9	0.122	0.512965	0.000004	6.4	0.512965
912DH	Basalt	79.0	923	0.236	0.248	0.703203	0.000009	0.70320	6.66	33.8	0.120	0.512967	0.000006	6.4	0.512967
914DH	Basalt	81.2	917	0.236	0.257	0.703186	0.000008	0.70319	6.57	34.1	0.117	0.512948	0.000004	6.0	0.512948
916DH	Basalt	79.9	966	0.236	0.240	0.703119	0.000011	0.70312	6.84	35.8	0.116	0.512958	0.000005	6.2	0.512958
918DH	Basalt	87.3	1000	0.236	0.253	0.703163	0.000011	0.70316	8.07	41.8	0.117	0.512949	0.000003	6.1	0.512949
932DH	Basalt	76.2	999	0.236	0.221	0.703067	0.000008	0.70307	7.32	39.0	0.114	0.512971	0.000004	6.5	0.512971
933DH	Basalt	79.2	1010	0.236	0.227	0.703085	0.000007	0.70308	7.64	39.1	0.118	0.512967	0.000004	6.4	0.512967
937DH	Basalt	80.3	1008	0.236	0.231	0.703091	0.000011	0.70309	7.25	38.6	0.114	0.512958	0.000004	6.2	0.512958
919DH	Dacite	156	429	18	1.056	0.710634	0.000008	0.71036	4.38	19.8	0.134	0.512366	0.000005	-5.2	0.512350
920DH	Dacite	120	691	18	0.502	0.710951	0.000007	0.71082	4.39	19.2	0.139	0.512408	0.000008	-4.4	0.512392
820DH	Dacite	126	317	18	1.150	0.710059	0.000008	0.70977	4.85	25.0	0.117	0.512263	0.000004	-7.1	0.512249
821DH	Dacite	125	311	18	1.163	0.710015	0.000007	0.70972	4.92	26.2	0.114	0.512268	0.000004	-7.0	0.512255
822DH	Dacite	117	334	18	1.014	0.710257	0.000007	0.71000	4.95	26.7	0.112	0.512254	0.000004	-7.3	0.512241
824DH	Dacite	118	293	18	1.166	0.710298	0.000009	0.71000	5.34	28.7	0.113	0.512266	0.000005	-7.1	0.512253
922DH	Dacite	138	216	18	1.850	0.710580	0.000009	0.71011	5.63	29.5	0.116	0.512255	0.000004	-7.3	0.512241
924DH	Dacite	113	290	18	1.128	0.710329	0.000008	0.71004	4.83	23.0	0.127	0.512263	0.000005	-7.2	0.512248
927DH	Dacite	117	307	18	1.108	0.710319	0.000009	0.71004	5.10	25.9	0.120	0.512259	0.000005	-7.2	0.512245
928DH	Dacite	114	268	18	1.229	0.710325	0.000007	0.71001	4.67	23.3	0.122	0.512270	0.000005	-7.0	0.512256
929DH	Dacite	118	285	18	1.203	0.710293	0.000008	0.70999	4.67	21.9	0.130	0.512264	0.000005	-7.1	0.512249
930DH	Dacite	134	220	18	1.760	0.710547	0.000009	0.71010	4.89	24.1	0.123	0.512257	0.000004	-7.3	0.512242
Standard								Recommended value							Recommended value

BCR-2	0.704997	0.000008	0.705026[1]	0.512648	0.000005	0.512638[1]	0.000015[1]
RGM-2	0.704146	0.000011	0.704184[1]	0.512816	0.000004	0.512803[2]	

1. Weis, D., Kieffer, B., Maerschalk, C., Barling, J., Jong, J. D., Williams, G. A., et al. (2006). High-precision isotopic characterization of usgs reference materials by tims and mc-icp-ms. Geochemistry Geophysics Geosystems, 7(8), 139-149.
2. Li, C. F., Li, X. H., Li, Q. L., Guo, J. H., & Yang, Y. H. (2012). Rapid and precise determination of sr and nd isotopic ratios in geological samples from the same filament loading by thermal ionization mass spectrometry employing a single-step separation scheme. Analytica Chimica Acta, 727(10), 54-60.